The Primary Breakup of Sonic & Supersonic Air-Assist Atomizers

Raghav Sikka*[1], Joachim Lundberg[1], Knut Vågsæther[1], Dag Bjerketvedt[1]
[1] Faculty of Technology, Natural Sciences, and Maritime Sciences
University of South-Eastern Norway, Porsgrunn, Norway
*Corresponding author email: Raghav.sikka@usn.no

Abstract
The present study compares twin-fluid atomizers novel concepts based on the airflow (shock waves) pattern obtained through Shadowgraph Imaging. The research work was conducted using the backlight imaging technique for converging (sonic) and converging-diverging (supersonic) air-assist atomizer with a 3.0 mm (throat) diameter. An annular sheet of thicknesses 70 µm and 280 µm with a high-speed air-core was employed to study the breakup dynamics for the different water mass flow rates (100 - 350 kg/hr) and air mass flow rates (5 - 35 kg/hr). Different sheet breakup patterns were identified as the function of the ALR ratio (air-to-liquid mass flow), liquid Weber number (We_l), and gas Reynolds number (Re_g). Different breakup modes extend from canonical Rayleigh bubble breakup, ligament-type breakup to the pure pulsating breakup via annular sheet disintegration. Spray angle variation was also observed with the change in sheet thickness and underexpanded flow and overexpanded flow in the converging and converging-diverging (CD) air-assist atomizers, respectively, due to the drastic difference in the jet flow dynamics.

Keywords
Sonic air-assist Atomizers, Primary breakup, Breakup morphology, Annular sheet

Introduction

The twin-fluid atomization is widely used, especially for heavy (viscous) Newtonian fluids or Non-Newtonian fluids. Its main attribute is low-pressure requirements than the mechanical counterpart, at the expense of an external source of atomizing fluid (air) for high**-**speed twin-fluid interaction. Earlier studies showed that a sheet is optimal for good atomization than a jet breakup [1]. Many researchers studied the sheet breakup mainly in two types – flat sheets or annular sheets. Though, flat sheets have gained more attention in the early days due to their classical problem structure. Lately, the annular sheet also received quite attention. Two major distinctions were thoroughly studied- inner air and outer air configuration, in which inner air is proven more effective in promoting sheet instability [2] & [3].

Based on the inner/outer air velocity or momentum, many modes or breakup patterns were identified. Kawano et al. [4] investigated the sheet breakup and found two modes based on a critical air velocity – *liquid lump and liquid film*. Choi et al. [5] observed three breakup modes – *Rayleigh, bubble-breakup, and pure-pulsating* depending on relative air and liquid rates. A photographic investigation by Adzic et al. [6] categorized breakup into *Kelvin-Helmholtz (a new regime – christmas tree), cellular, and atomization*. Three flow regimes for the annular jet breakup process have been identified, i.e., bubble formation, annular jet formation, and atomization by Li et al. [7]. Ligament spacing is wider for thick sheets, especially in an annular sheet case investigated by Berthoumieu et al. [8]. Leboucher et al. [3,9] thoroughly studied the breakup based on air-liquid momentum and found modes such as *rayleigh, bubble, christmas tree, pure pulsating*. Zhao et al. [10] discerned the breakup modes – *bubble, christmas tree (cellular), and fiber breakup* based on the morphological differences. But these studies are all done without taking into consideration the air-assist mechanism. Kihm et al.

[11,12] first investigated the sonic atomization concept to study effective atomization with liquid jet using shock waves dynamics in underexpanded or overexpanded flows. Though Sauter mean diameter decreases after the advent of shock patterns, it still questioned the use of supersonic jet with the aim of optimal atomization. This study aims to discern the various breakup modes or patterns in the light of effective atomization using sonic and supersonic flow, as they both depict different shock dynamics. This paper contains the experimental findings using a novel concept of sonic atomization employing an annular liquid sheet, whereas earlier studies employed a two-dimensional sheet [11] or jet [13]. Different breakup modes of the liquid sheet with co-flow air were observed subjected to different air and water flow rates (air-to-liquid ratio (ALR)). Spray angle variation was also investigated with different sheet thickness using converging and converging-diverging (CD) nozzle.

Experimental Method

The experimental schematic setup is shown below (see **Figure 1 a**). The atomizers tested were of two types – converging and converging-diverging (CD) air-assist atomizers with core airflow (3.0 mm throat diameter) and liquid (water) was injected through an annular gap (coaxial arrangement), which were connected at the end of the lance mounted onto the traversing system (**Figure 1 b**).

To study the sheet breakup, two different sheet thicknesses, 70 µm and 280 µm, were employed to examine sheet velocity (momentum) effects at employed flow rates. A pump supplied the liquid after passing through a filter. The liquid mass flow rate was regulated by altering the frequency of the pump, which was recalibrated for a given mass flow rate. The air was drawn through an in-house installed compressor with a maximum capacity of up to 100 psi (7 bar(g)). The Coriolis type flowmeter was used for both air and water flow rate measurements. The spray ejected out of the atomizer was collected in a box container; after that, it was again pumped to the injector through the hose.

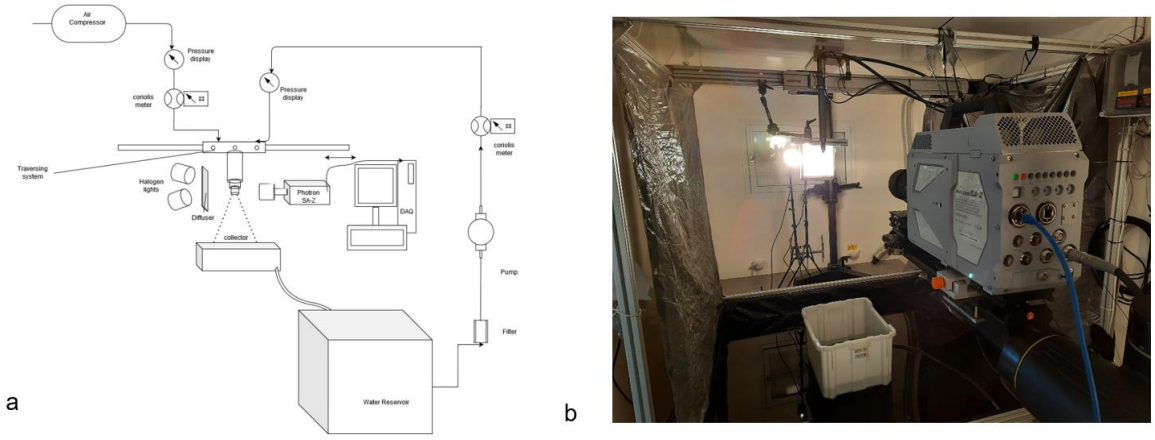

Figure 1. a) Schematic of Experimental Setup and b) Nozzle assembly with Backlighting (halogen light).

The backlight imaging method was adopted to provide the necessary insight into the near-nozzle dynamics. Two halogen lights (dedolight), 250 W each, and the diffuser screen were used to provide a diffused uniform background for the image acquisition. Photron CMOS-based high-speed camera SA-Z model was employed to capture the images at the frame rate of 8,000 frames per second with a shutter speed of 125 µs. However, it is not enough to capture instantaneous images at higher flow rates as per the Nyquist sampling criterion, but

good enough for the primary breakup study. The liquid flow rate varied from 100 kg/hr to 350 kg/hr, whereas the airflow rate varied from 1 kg/hr to 35 kg/hr, which corresponds to the air-to-liquid ratio (ALR) ranging from 0.00285 to 0.35. The main objective is to examine the effect of sonic (converging) or supersonic (CD) air-assist atomizer on the annular sheet breakup and the resulting spray pattern. The major difference in both types of nozzles is that converging type nozzle after the nozzle is choked develops the underexpanded sonic jet ($p_{exit} > p_{ambient}$), which forms a Prandtl-Meyer expansion fan at inception. In contrast, the CD nozzle goes through overexpansion ($p_{exit} < p_{ambient}$), resulting in the initial formation of oblique shock waves. Thus, both configurations belong to a unique class that may result in entirely different breakup characteristics for the novel atomizer. A series of experiments with varying flow rates were performed to find which configuration is more suitable for better primary atomization capability.

Experimental Results and Discussion

The primary breakup mechanism for the two kinds of atomizers tested was conjectured to be different due to the distinct jet characteristics. In the converging nozzle, an underexpansion flow pattern is shown in **Figure 2,** which results in the Prandtl-Meyer expansion waves [14] may try to deflect the liquid sheet in and out of the centerline, thus delaying the sheet contraction effect (due to the surface tension) even at low liquid flow rates. Besides, it prompts annular sheet to form instability waves on the inner side which gradually does sheet thinning at the wave trough, through which half waves are torn off through liquid sheet (like planar) when wave amplitude reaches a critical threshold forming ligaments, which further disrupts to form large globules/droplets depending on the aerodynamic interaction between high-speed jet air and ligaments.

In the converging-diverging nozzle (CD), which undergoes overexpansion (see **Figure 2**) for the higher airflow rates employed, thus forming the oblique shock waves with high interface strength of the jet boundary. This jet boundary interface strength might play two roles- firstly, forming sufficiently high amplitude unstable waves (Kelvin-Helmholtz instability) on the sheet surface.

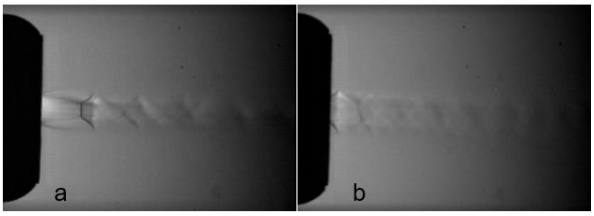

Figure 2. Shock waves pattern observed in Shadowgraph Imaging at 20,000 fps for a) converging nozzle and b) CD nozzle at 35 kg/hr airflow.

Secondly, the irregular pressure distribution due to the alternate compression and expansion of air-jet may drive the sheet into sudden acceleration and sudden retardation, which corresponds to the alternate sheet deflection towards and away from the centerline of the jet; thus irregular shaped liquid parcels might tear off from the sheet. The length of the sonic jet region can also affect the primary breakup, which eventually affects secondary atomization [13]. Also, wave growth and ligament formation depend mainly on the surface tension force, aerodynamic forces, which define the droplet size formation further downstream. The *bursting effect* (see **Figure 3**) was seen in both these cases at the neck formation region (which is formed early in converging atomizer due to flow behaviour). In general, for both cases, the neck bursting frequency varies depending on the aerodynamic interaction effects and the

natural pulsating frequency of the liquid sheet, and also pulsations caused due to slight variation in airflow rates (<2%). For the 70µm sheet, due to higher axial momentum, the breakup length (a) is longer than the 280 µm sheet (e). With increasing ALR, the mist-like droplets (tiny) formed downstream axially in 70 µm case (c & d) whereas some threads-like droplets (bigger) ejecting laterally out of the sheet can be visible with 280 µm sheet thickness (g & h). The sheet formed was corrugated/wavy in both the above cases forming a *cellular pattern* (whose cell size may depend upon the jet velocity), as well as *stretched-sheet/ligament structure both spanwise and streamwise direction* (both observed in planar sheet configuration [15,16]) which is attributed to the three-dimensional (3-D) nature of the annular sheet.

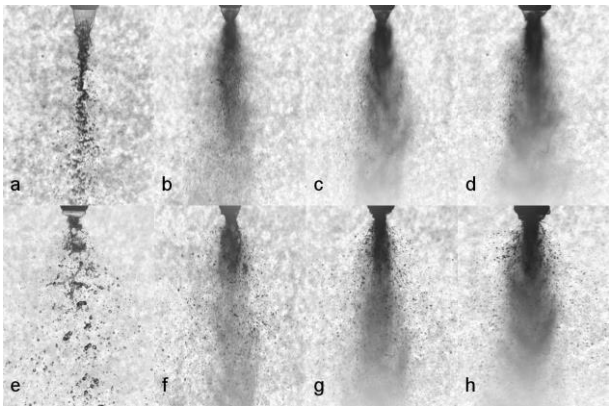

Figure 3. For converging-diverging nozzle with 70 µm (top row) & 280 µm (bottom row) sheet thickness at 100 kg/hr water flow rate with airflow rates a) & e) 5 kg/hr, b) & f) 15 kg/hr, c) & g) 25 kg/hr and d) & h) 35Kg/hr, respectively.

The pressure difference and the surface tension effect, and aerodynamic forces dictate the breakup characteristics of the liquid sheet, such as breakup length, spray angle etc.

1. Breakup dynamics

Different breakup patterns were observed for various flow rates such that at low flow rates, the *Rayleigh bubble regime* (a) was found with a certain bubble formation frequency at a given airflow rate (see **Figure 4**).

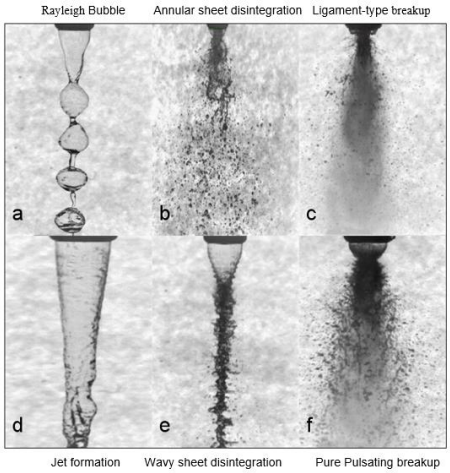

Figure 4. For converging nozzle with 280 µm sheet thickness at 100 kg/hr water flow rate (Top row) & at 350 kg/hr water flow rate (Bottom row), respectively; with airflow rates a) & d) 1 kg/hr, b) & e) 10 kg/hr, and c) & f) 35Kg/hr, respectively.

With a slight increase in airflow rates, *the bubble breakup* regime, as observed in [5], was visualized, forming ligaments and large globular droplets downstream. With further increase in air mass flow rates or ALR, the aerodynamic interaction increases, leading to corrugated/wavy sheet contraction, forming a neck region where the bursting phenomenon was identified. This bursting occurs near the nozzle exit region, forming the *annular sheet disintegration regime* (b). With further increase in ALR, the ligaments/filaments shed directly from the near-nozzle region due to the very high-speed interaction lead to a regime known as *ligament-type breakup* (c). As we increase liquid flow rates at low ALR, the *jet formation (d)* occurs with some waviness. With further increase in ALR, the wavy sheet was formed near the nozzle, which is contracted to form a *wavy sheet disintegration* (e), which leads to ligaments interconnected in a three-dimensional fashion along with satellite drops downstream. At high flow rates (ALR), ligaments shed from all azimuthal angles of the annular sheet neck region, forming a christmas-tree like regime. Finally, at very high air-liquid flow rates (ALR), a *pure-pulsating regime* (f) almost similar to the 'christmas tree breakup' observed as in [9], in which ligament-like structures pulsates alternatively on the left and right side of the spray centreline.

The breakup modes or regime diagram (see **Figure 5**) for both converging and converging-diverging (CD) atomizer is quite similar, with a slight variation in the ALR range for different regimes.

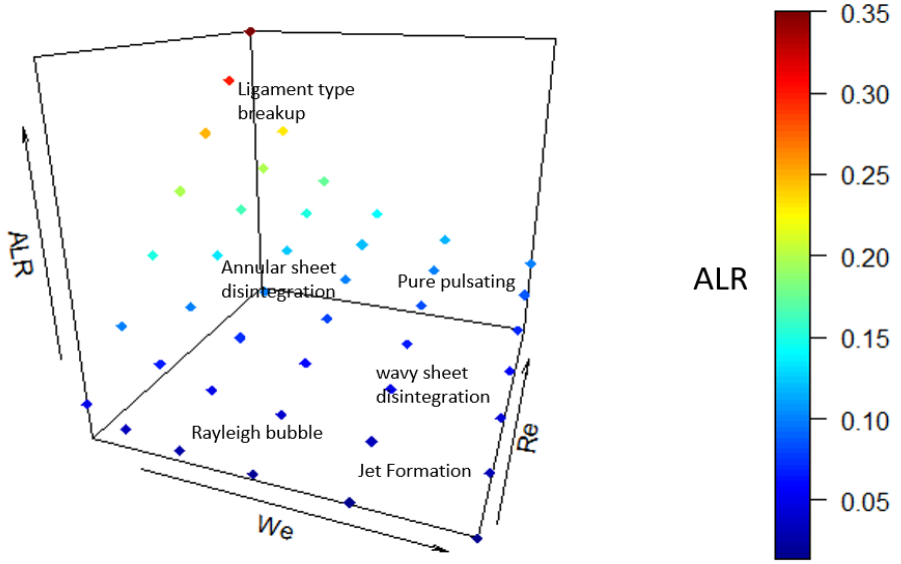

Figure 5. Regime diagram for the converging nozzle atomizer for various flow rates for 280 µm sheet thickness.

It is plotted for converging nozzle atomizer case for 280 µm sheet thickness based on the air-to-liquid ratio (ALR) along with the non-dimensional numbers, Eq (1) as Reynolds number Re_g and Eq (2) as Weber number We_l, defined respectively, such that assuming dynamic viscosity of air to be a relatively constant value of 18 µPa.s at 15 ° C.

$$Re_g = \rho_g u_g d / \mu_g \quad (1)$$

$$We_l = \rho_l u_l^2 t / \sigma_l \quad (2)$$

l= liquid, *g* = gas (air)

Where *d*: air orifice (throat) diameter, *t*: sheet thickness

2. Spray angle Variation

The spray angle variation was observed for change in fluid flow rates. Spray angle measurement is based on the tangent lines fitted at the spray edges at some downstream location, but the spray periphery is curved due to air-interaction effects. In our case, spray angle was measured such that it covers the majority (approximately 99 %) of the droplet mass of the whole spray as is depicted (see **Figure 6 a & b**). The set of 25 images (frames) were pre-processed (sharpness and contrast enhancement) in the *ImageJ* software for each data set before the angles measurements were taken. The angles were obtained by taking the mean (average) value of these 25 images with an uncertainty of 2-3% due to observation error as the spray boundary line is vague. The intensity-averaged images (**Figure 6 c & d**) were not taken for measurement as it underpredicts the spray angle for most cases.

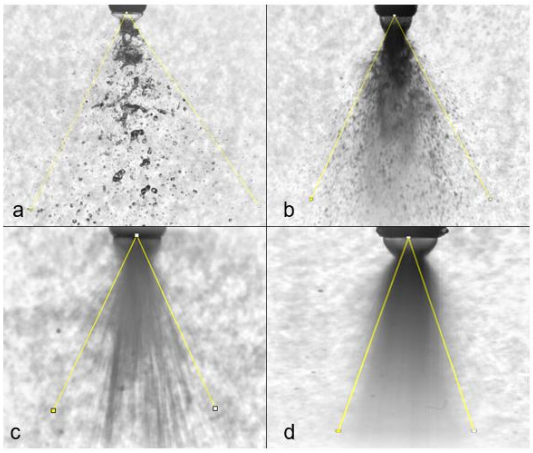

Figure 6. Spray angle measurement for CD nozzle atomizer for two cases a) & c) water and an airflow rate of 100 kg /hr and 5 kg/hr, respectively, b) & d) water and an airflow rate of 350 kg/hr and 35 kg/hr, respectively.

For both 70 µm and 280 µm sheets, the spray angle is plotted against the water flow rate (see **Figure 7 a & b**). For higher airflow rates (say,15 kg/hr), as the water flow rate increases, the spray angle decreases rapidly for a thinner sheet (70 µm), whereas the spray angle slightly increases then decreases for a thicker sheet (280 µm) due to the prompt increase in liquid axial momentum in the former case.

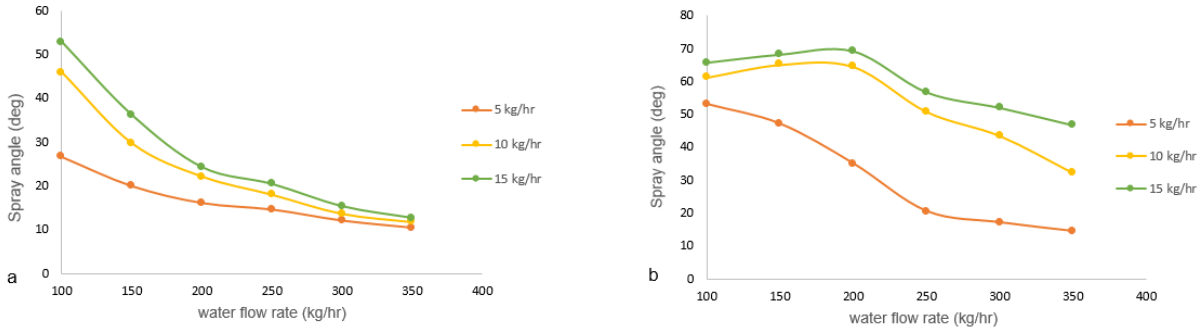

Figure 7. Spray angle measurement for converging-diverging (CD) atomizer for a) 70 µm sheet and b) 280 µm sheet thickness.

For a lower airflow rate (say, 5 kg/hr), the spray angle decreases continuously in both 70 µm and 280 µm sheet thickness. The relatively larger spray angle in the thicker sheet than the

thin sheet case is attributed to the lower axial momentum of the thicker liquid sheet, despite the sheet contraction effect. At low air and water flow rates, the spray angle is almost identical in both converging atomizer and CD atomizer for 280 µm sheet thickness (**Figure 8 a**) due to the slight contraction effect subjected to the absence of waves pattern. Whereas at higher airflow rates, the spray angle is larger in the CD atomizer than the converging atomizer, which might be due to the alternate contraction and expansion of the sheet due to high liquid-air interface strength attributed to the advent of waves pattern. Also, the bursting effect is more pronounced in CD than in the converging atomizer.

The spray angle is plotted against the ALR for 280 µm sheet thickness (**Figure 8 b**); the angle increases up to an ALR value of 0.28, then further reaches a plateau before slightly decreasing until 0.35 ALR value. The maximum spray angle reaches around the ALR value of 0.3 for both converging and CD atomizer. At higher flow rates, the momentum increases axially, which led to less divergence in the spray boundary in the near downstream region (where spray angle was measured). A 2nd-degree polynomial curve fit is also shown for both converging and converging-diverging (CD) atomizer.

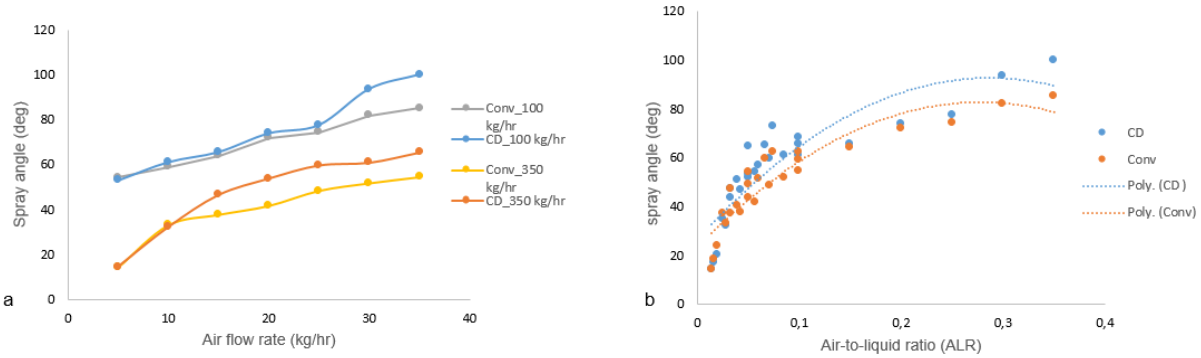

Figure 8. a) Spray angle comparison plotted against airflow rate and b) Spray angle measurement plotted against air-to-liquid ratio (ALR) for both converging atomizer and converging-diverging (CD) atomizer.

Conclusion

The characteristics of an annular sheet-based atomizer spray were photographically analyzed using high-speed imaging to study the breakup dynamics for the distinct airflow mechanism – the converging and the CD atomizer. Breakup modes were discerned in both converging and CD atomizer with a sheet thickness of 280 µm. From canonical Rayleigh bubble formation at very low ALR values, the annular sheet disintegration, the ligament-type breakup at very high ALR values, various modes were obtained. The jet formation occurs at high liquid flow rates, whereas wavy sheet disintegration occurred at some moderate ALR values when the sheet contracted to form inter-connected ligament-like structures convecting in 3D space. The higher flow rates result in the formation of the christmas-tree breakup pattern.

Furthermore, the pure-pulsating mode was observed with the ligaments convecting downstream axially in alternate left and right direction pulsations to the spray centerline with a further increase in airflow rate. The spray angle was also obtained using the *ImageJ* software-based analysis. The spray angle shows a declining pattern with the increase in water flow rates (due to increased axial momentum) for both 70 µm and 280 µm sheet thickness, whereas the spray angle increases monotonously with an increase in airflow rates, for both converging and CD atomizers, respectively with 280 µm sheet thickness. The increment in spray angle is more in CD atomizers than in the converging atomizer at higher airflow rates due to the more pronounced bursting effect in the former case.

Nomenclature

d	air orifice (throat) diameter [mm]		Greek symbols
t	sheet thickness [µm]	μ	viscosity [$Ns \cdot m^{-2}$]
We_l	Weber number	ρ	density [$kg \cdot m^{-3}$]
Re_g	Reynolds number	σ	surface tension [$N \cdot m^{-1}$]
U	Velocity [$m \cdot s^{-1}$]		

References

[1] Leboucher, N., Laporte, G., and Carreau, J. L., 2007, "Effect of the Inner Gas Jet on Annular Liquid Sheet Atomization," 21st ILASS- Europe Meeting, pp. 1–5.

[2] Fu, H., Li, X., Prociw, L. A., and Hu, T. C. J., 2003, "Experimental Investigation on the Breakup of Annular Liquid Sheets in Two Co-Flowing Airstreams," 1st International Energy Conversion Engineering Conference IECEC, (August), pp. 1–11.

[3] Leboucher, N., Roger, F., and Carreau, J. L., 2010, "Disintegration Process of an Annular Liquid Sheet Assisted by Coaxial Gaseous Coflow(S)," Atomization and Sprays, **20**(10), pp. 847–862.

[4] Kawano, S., Hashimoto, H., Togari, H., Ihara, A., Suzuki, T., and Harada, T., 1997, "Deformation and Breakup of an Annular Liquid Sheet in a Gas Stream," Atomization and Sprays, **7**(4), pp. 359–374.

[5] Choi, C. J., 1997, "Disintegration of Annular Liquid Sheet with Core Air Flow -Mode Classification," International journal of fluid mechanics research, **24**(1–3), pp. 399–406.

[6] Adzic, M., Carvalho, I. S., and Heitor, M. V, 2001, "Visualization of the Disintegration of an Annular Liquid Sheet in a Coaxial Air-Blast Injector at Low Atomizing Air Velocities," Optical Diagnostics in Engineering, **5**(1), pp. 27–38.

[7] Li, X., and Shen, J., 2001, "Experiments on Annular Liquid Jet Breakup," Atomization and Sprays, **11**, pp. 557–573.

[8] Berthoumieu, P., and Lavergne, G., 2001, "Video Techniques Applied to the Characterization of Liquid Sheet Breakup," Journal of Visualization, **4**(3), pp. 267–275.

[9] Leboucher, N., Roger, F., and Carreau, J. L., 2012, "Characteristics of the Spray Produced by the Atomization of an Annular Liquid Sheet Assisted by an Inner Gas Jet," Atomization and Sprays, **22**(6), pp. 515–542.

[10] Zhao, H., Xu, J. L., Wu, J. H., Li, W. F., and Liu, H. F., 2015, "Breakup Morphology of Annular Liquid Sheet with an Inner Round Air Stream," Chemical Engineering Science, **137**, pp. 412–422.

[11] Kihm, K. D., and Chigier, N., 1991, "Effect of Shock Waves on Liquid Atomization of a Two-Dimensional Airblast Atomizer," Atomization and Sprays, **1**(1), pp. 113–136.

[12] B.K.Park, J.S.Lee, and K.D.Kihm, 1996, "Comparative Study of Twin-Fluid Atomization Using Sonic or Supersonic Gas Jets," Atomization and Sprays, **6**, pp. 285–304.

[13] Mates, S. P., and Settles, G. S., 2005, "A Study of Liquid Metal Atomization Using Close-Coupled Nozzles, Part 2: Atomization Behavior," Atomization and Sprays, **15**(1), pp. 41–59.

[14] Zapryagaev, V., Kiselev, N., and Gubanov, D., 2018, "Shock-Wave Structure of Supersonic Jet Flows," Aerospace, **5**(2).

[15] B. E. Stapper, 1992, "An Experimental Study of the Effects of Liquid Properties on the Breakup of a Two-Dimensional Liquid Sheet," Journal of Engineering for Gas Turbines and Power, **114**(1).

[16] Lavergne, G., Trichet, P., Hebrard, P., and Biscos, Y., 1993, "Liquid Sheet Disintegration and Atomization Process on a Simplified Airblast Atomizer," Journal of Engineering for Gas Turbines and Power, **115**, pp. 461–466.